Analysis of intraocular lens surface adhesiveness by atomic force microscopy

Marco Lombardo, MD, PhD, Giovanni Carbone, PhD, Giuseppe Lombardo, Eng, PhD, Maria P. De Santo, PhD, Riccardo Barberi, PhD

PURPOSE: To analyze intraocular lens (IOL) optic surface adhesiveness using atomic force microscopy (AFM).

SETTING: LiCryL Laboratory, University of Calabria, Rende, Italy.

METHODS: The surface adhesive properties of poly(methyl methacrylate) (PMMA), silicone, hydrophilic acrylic, and hydrophobic acrylic IOLs were evaluated by AFM. Analysis was performed at room temperature (21°C) in a liquid environment using the force-versus-distance mode of a commercial instrument (NanoScope III). Measurements were acquired with rectangular silicon cantilevers of a nominal elastic constant of 10 Newton/m. The nominal value of the tip's radius of curvature was 1 μm, and the scanning speed during the acquisitions ranged from 10 to 400 nm/s.

RESULTS: The adhesion force measurements showed different characteristics for the various types of IOLs ($P<.001$, analysis of variance). The hydrophobic acrylic IOL had the largest mean adhesive force (283.75 nanoNewton [nN] ± 0.14 [SD]) followed by the hydrophilic acrylic (84.76 ± 0.94 nN), PMMA (45.77 ± 0.47 nN), and silicone (2.10 ± 0.01 nN) IOLs.

CONCLUSIONS: The surface properties of the biomaterials used to manufacture IOLs are important because they can influence the incidence and severity of posterior capsule opacification (PCO). Although further studies are necessary to elucidate the mechanism of PCO development and the interface interactions between the IOL and capsule, the results in this study may bolster the theory of manufacturing more-adhesive materials to prevent PCO.

J Cataract Refract Surg 2009; 35:1266–1272 © 2009 ASCRS and ESCRS

During the past decade, cataract patients have benefited from substantial improvements in phacoemulsification systems and fluidics and new intraocular lens (IOL) design and materials. Nevertheless, posterior capsule opacification (PCO) remains a significant cause of visual impairment after surgery, with a mean incidence of approximately 5% a mean of 3 years after surgery.[1–4] Various surgical strategies to minimize the risk for PCO have been proposed.[5–7] Nevertheless, prevention of PCO is mainly attributed to the development of new IOL materials and IOL optic designs.[8]

Posterior capsule opacification is thought to have a multifactorial pathogenesis, and lens epithelial cells (LECs) are considered to be the main cellular precursors of this process.[9] The LECs lie immediately adjacent to the inner surface of the lens capsule and remain attached to the capsular bag after cataract extraction. These cells can proliferate and migrate into the space between the IOL and the lens capsule, leading to capsule opacification.[10] Inflammatory cells can contribute to the development of PCO by activating LEC migration and promoting their proliferation and migration.[11,12]

Because the type or design of the IOL biomaterial has great influence on the inflammatory reaction and LEC behavior after IOL implantation,[13] much research has been performed to analyze which IOL property primarily influences the adhesion and migration of LECs onto the IOL optic and in the space between the IOL and capsule. A sharp posterior optic edge design of an IOL is reported to be a major factor in the prevention of PCO.[2,14–16] By pressing against the posterior capsule, the square-edge component creates a discontinuous capsular bend as the anterior and posterior capsules adhere together. This is thought to serve as a physical barrier to the migration of LECs. However, many authors have pointed out the importance of the IOL biomaterial in preventing PCO after they found that acrylic IOLs and silicone

0886-3350/09/$—see front matter
doi:10.1016/j.jcrs.2009.02.029

IOLs caused less PCO than conventional poly(methyl methacrylate) (PMMA) IOLs.[17–20] Despite these extensive studies, the mechanism by which the IOL material influences LEC behavior remains controversial.[21] Undoubtedly, a sharp optic edge alone cannot provide a substantial barrier when a capsular bend is not formed.[22,23] Hence, fast and firm capsule adhesion could be a prerequisite to capsular bend formation.

Because the chemicophysical properties of the IOL optic surface are the main factors that influence interfacial interactions between the IOL and the lens capsule environment, LEC behavior may be greatly influenced by the surface properties of the IOL, such as the morphology or adhesiveness.

In a previous study,[24] we evaluated the surface topography of various types of IOLs using atomic force microscopy (AFM). We found different features with respect to the IOL biomaterial and measured a smoother optic surface on acrylic and silicone IOLs than on PMMA IOLs. The amount of surface irregularities is related to the number of inflammatory cells and LECs adhering to the optic surface of the IOL,[25] with a polished surface playing an important role in reducing the rate of cell migration.

The purpose of the present study was to broaden our knowledge of the submicron surface properties of IOLs by analyzing the adhesiveness of 4 IOL optic materials using AFM.

MATERIALS AND METHODS

The following 4 types of posterior chamber IOLs were examined: 1-piece PMMA, second-generation 3-piece silicone, 1-piece hydrophilic acrylic, and 3-piece hydrophobic acrylic. Table 1 shows the IOL specifications. The range of refractive power was between 17.0 diopters [D] and 25.0 D for all IOLs tested. Before the measurement was performed, each IOL was removed from its sterile pack with an atraumatic forceps and placed on a purpose-designed Teflon environmental cell. The sample was held by a steel spring with the anterior surface optic side facing downward.

The adhesion properties of IOLs were measured using a commercially available atomic force microscope (NanoScope III, Veeco) in the force-versus-distance (*f-d*) mode.[26,27] To avoid capillarity and double-layer forces, adhesion measurements were performed at room temperature (21°C) in deionized water (Figure 1) using rectangular silicon cantilevers of a nominal elastic constant of 10 Newton/m (Nanoandmore GmbH).[28] The nominal value of the tip's radius of curvature was 1 μm, and the scanning speed during the acquisitions ranged from 10 to 400 nm/s. It was verified that in this range, the measurements were independent of the scanning rate. A probe with a micrometer-sized tip was chosen 2 reasons. First, a large radius of curvature allows better precision in determining the adhesive forces. Second, a large radius helps prevent damage to the sample.

In the *f-d* mode of AFM, forces applied on the sample's surface are measured by the deflection of the cantilever while approaching and retracting from the sample's surface. In this study, the force measurement relied on the IOL sample being repeatedly approached toward and retracted away from the tip. In the extension–retraction cycle, a signal proportional to the deflection of the cantilever (Z) is recorded as a function of the vertical position (D) of the piezoelectric stage. To transform the arbitrary deflection of the cantilever into an *f-d* curve, the position-sensitive detector sensitivity should be known; it can be determined as the slope of the curve in the contact region, as shown in Figure 2. Then, Z can be converted into units of force (nanoNewton [nN]) according to Hooke's law: $F = k_c \times Z$, where k_c is the cantilever elastic constant. The probe–sample separation d is then evaluated as the sum of the piezo displacement and the cantilever deflection as follows: $d = D + Z$. A routine was implemented using MatLab software (version 7.0, The MathWorks, Inc.) to convert the AFM raw deflection data (D and Z) into a force profile.

Table 1. Intraocular lens optic specifications.

IOL Material	IOL Model (Manufacturer)/Specifications
PMMA	102 C (Soleko)/6.50 mm disk optic; biconvex; rigid; UV absorbing; posterior chamber
Silicone	911A CeeOn Edge (Pharmacia)/6.00 mm optic; biconvex; foldable; UV absorbing; posterior chamber
Hydrophilic acrylic	Akreos Fit (Bausch & Lomb)/5.75 mm disk optic; biconvex; foldable; posterior chamber
Hydrophobic acrylic	Model MA60AC (Alcon Labs)/6.00 mm disk optic; biconvex; foldable; UV absorbing; posterior chamber

IOL = intraocular lens; PMMA = poly(methyl methacrylate); UV = ultraviolet

Submitted: December 30, 2008.
Final revision submitted: February 4, 2009.
Accepted: February 6, 2009.

From Vision Engineering (M. Lombardo, G. Lombardo), Rome, and Reggio Calabria, CEMIF. CAL, CNR-INFM LiCryL Laboratory, Physics Department, University of Calabria, Rende (M. Lombardo, Carbone, G. Lombardo, De Santo, Barberi), Italy; the Department of Engineering Science (Carbone), University of Oxford, Oxford, United Kingdom.

No author has a financial or proprietary interest in any material or method mentioned.

Presented at the annual meeting of the Association for Research in Vision and Ophthalmology, Fort Lauderdale, Florida, USA, May 2009.

Innova Technology Solutions, Chieti, Italy, provided the consumables.

Corresponding author: Marco Lombardo, MD, PhD, Via Adda 7, 00198 Rome, Italy. E-mail: mlombardo@visioeng.it.

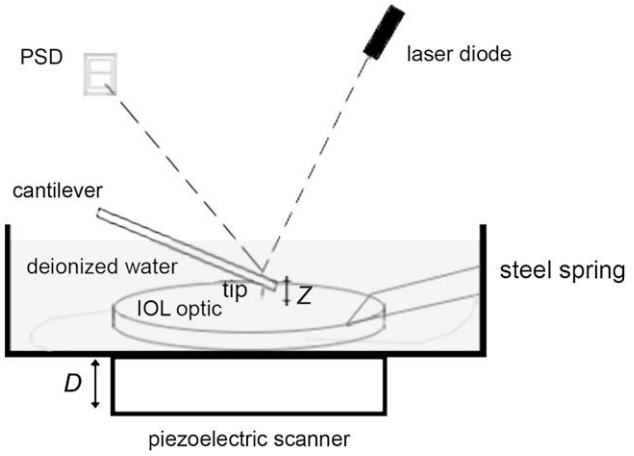

Figure 1. The AFM can probe nanomechanical properties, such as stiffness or adhesion, on a sample's surface by generating force curves. Force curves measure nN-range vertical forces applied to the surface and are generated by performing controlled vertical tip-sample interactions. The position of the sample is adjusted by the piezoelectric translator. The deflection of the cantilever is usually measured using the optical lever technique. A beam from a laser diode is focused on the end of the cantilever. The position of the reflected beam is monitored by a position-sensitive detector (PSD). To avoid the meniscus force that would otherwise dominate Van der Waals and any other weaker interaction, the sample and the tip have to be immersed in liquid. In this study, deionized water was used to minimize the effect of double-layer forces. These repulsive forces are due to the charging of the sample and the tip surfaces, which in water is caused by adsorption of ions from the solution onto the surface and by the dissociation of functional groups on the surface. To highlight details, the figure was not scaled (D = vertical position of the piezoelectric stage; IOL = intraocular lens; Z = deflection of the cantilever).

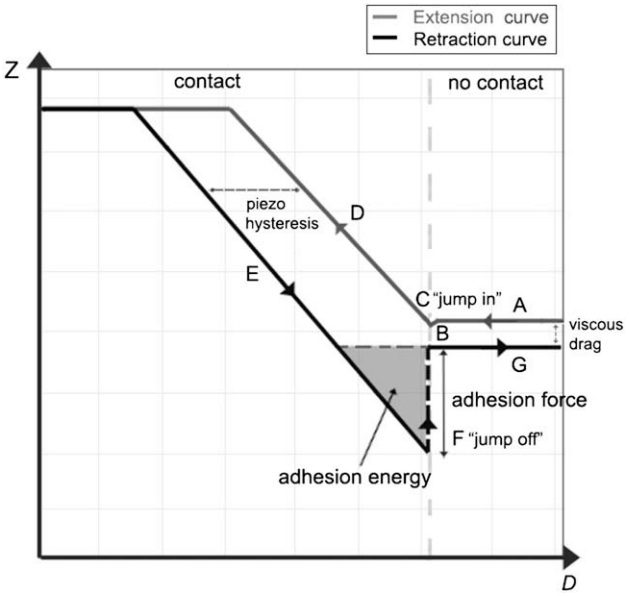

Figure 2. Graphical representation of an *f-d* curve. *A*: At large separation, the interaction between the sample and probe is zero (no contact region). *B*: As the sample's surface approaches the probe, the cantilever may bend upward due to the repulsive forces (double-layer forces). *C*: The probe jumps into contact when the gradient of forces (attractive) exceeds the spring constant of the cantilever, k_c ("jump-in"). *D*: When the force is increased in the contact region, the shape of the approach curve may provide direct information on the material properties of the sample (eg, stiffness). *E*: On retraction of the sample's surface from the probe, the approach and retraction curves may not overlap due to the difference in the piezo displacement versus the applied voltage (piezo hysteresis). *F*: The tip and sample separate when the gradient of the adhesion forces becomes smaller than k_c ("jump-off") and the tip returns to its resting position (*G*). Contact and noncontact parts of the *f-d* curve are easily distinguishable. In an *f-d* plot, Z and D are the cantilever deflection and the piezo displacement, respectively.

Figure 2 is a schematic of an *f-d* curve during a full cycle. It consists of 2 parts: the approach and the withdrawal curve, which is acquired while the sample is moved vertically toward the tip and back. The extension (gray) curve in Figure 2 corresponds to the force measured while the probe approaches the sample (run-in); the retraction (black) curve represents the force measured while it is retracted (run-out). Each curve can be further divided into a no-contact region, where the probe–sample interaction is negligible and the cantilever deflection is zero; a contact region, where the probe is in contact with the sample surface; and an intermediate region (Figure 2, *dashed gray line*), where the probe and the sample are close to each other and the cantilever is deflected by van der Waals and electrostatic forces. Any difference between the approach and retraction is called *f-d* curve hysteresis. The hysteresis of the curve in Figure 2 shows 3 main features. The first is vertical offset in the no-contact region. It is only present when working in liquid and is mainly due to hydrodynamic drag on the cantilever, which produces a force in the direction opposite to the movement of the cantilever.[29] The second feature is horizontal offset in the contact region, which is caused by the hysteresis in the piezoelectric extension of the scanner[30] as well as by plastic and viscoelastic deformation of the sample surface.[31] The third feature is hysteresis in the intermediate region. This hysteresis is mainly due to the adhesive forces, which tend to keep the surfaces in contact. In the run-out, the elastic force of the cantilever has to work against adhesion to separate the probe from the surface (ie, the jump off).

The experimental conditions and parameters of the force measurement were chosen to eliminate the effect of hydrodynamic drag. Hysteresis in the piezoelectric extension of the scanner was still present but did not affect the interpretation of the data.

The adhesion between the probe and the IOL surface was measured from the minimum of the run-out. The difference between the minimum of this curve and the tip's resting position is proportional to the maximum adhesion force (F_{ad}). The adhesion energy (W_{ad}), equal to the gray area in Figure 2, was further measured.

For statistical analysis, the F_{ad} and W_{ad} values were calculated on 50 curves taken in the central region of the posterior optic of each analyzed IOL. All data used for statistical analysis were acquired using the same cantilever. This procedure was used to avoid bias that may have been introduced by the cantilever elastic constant calibration and the different probe radius. The 1-way analysis of variance (ANOVA) test was used to statistically compare the differences between IOL types in F_{ad} and W_{ad} values. When statistical significance was found, the differences between IOLs were further compared using the Tukey test for pairwise comparisons.

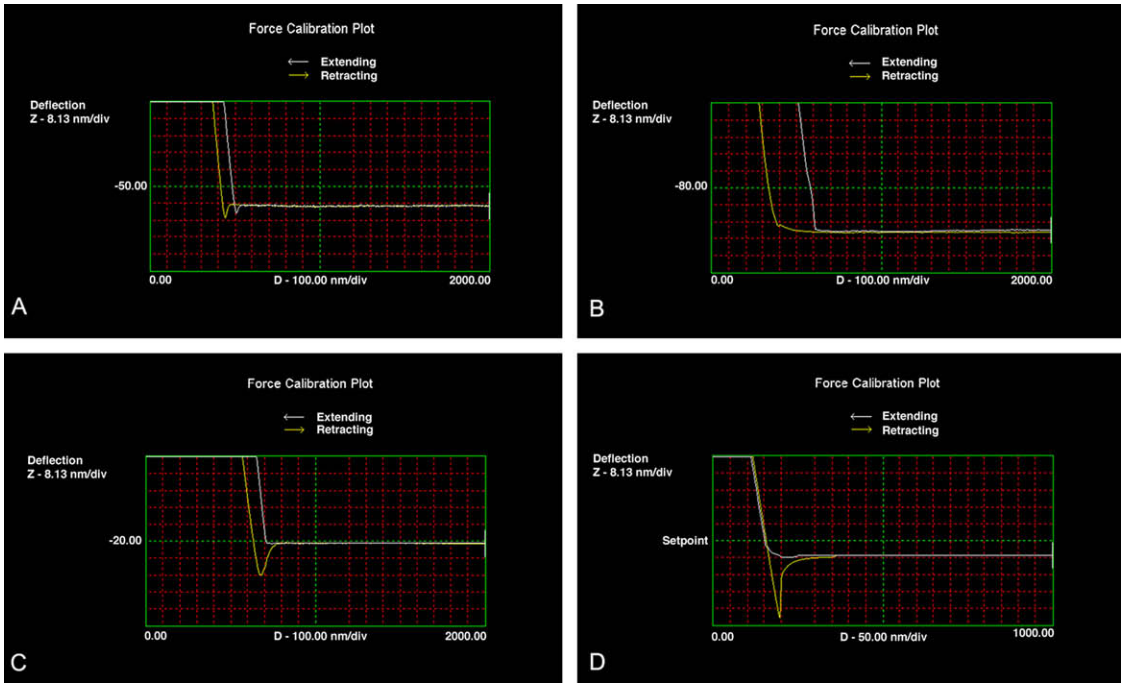

Figure 3. Force calibration plots of a typical extension–retraction cycle for each type of IOL material tested. *A*: Curves of PMMA IOL. *B*: Curves of silicone IOL. *C*: Curves of hydrophilic acrylic IOL. *D*: Curves of hydrophobic acrylic IOL. The sample displacement position (D) and the cantilever deflection (Z) are in the *x*-axis and *y*-axis, respectively. Knowing the position-sensitive detector sensitivity and k_c, F_{ad} can be calculated according to Hooke's law, as summarized in the text. No plastic or viscoelastic deformation of the sample surface has occurred. This was confirmed by the reproducibility of the data as well as the finding that both trace and retrace show the same slope in the contact region. The adhesiveness properties of the sample surface can be extracted from *f-d* curves by examining the response of the material to unloading. On retraction, the maximum cantilever deflection was observed for the hydrophobic acrylic IOL and the minimum for the silicone IOL.

Differences with a *P* value of 0.05 or less were considered statistically significant.

RESULTS

In the most general case, the adhesion force F_{ad} is a combination of the electrostatic force F_{el}, the van der Waals force F_{vdW}, the meniscus or capillary force F_{cap}, and forces due to chemical bonds or acid–base interactions, F_{chem}, where $F_{ad} = F_{el} + F_{vdW} + F_{cap} + F_{chem}$. In aqueous solutions, the F_{cap} is eliminated, as explained in the legend to Figure 1, and electrostatic forces become relatively more important because most surfaces are charged due to dissociation of surfaces groups. On the other hand, their magnitude depends on electrolyte concentration. Thus, using deionized water, one can greatly minimize their contribution, in addition to the contribution of F_{chem}. In this study, F_{vdW} made the largest contribution to F_{ad}.

Figure 3 shows the typical curves acquired for each IOL material. Table 2 shows the surface adhesion property results for each IOL. Values were significantly different between the IOLs of various materials ($P < .001$, ANOVA). The measured F_{ad} value was highest on the hydrophobic acrylic IOL, whereas the force curves on the silicone IOL had the smallest attraction between the tip and the sample's surface. A direct comparison of each pair of IOLs found statistically significant differences ($P < .001$, Tukey). The measured W_{ad} value was highest on the hydrophobic acrylic IOL and lowest on the silicone IOL.

Multiple *f-d* curves were recorded on different areas of the central posterior optic surface and always showed the same features, indicating that the IOL surface was homogeneous in terms of chemicophysical properties. Moreover, for each position, no

Table 2. Adhesion force and adhesion energy measurements calculated in the central region of the posterior optic surface of each type of IOL.

	Mean ± SD	
IOL Sample	Adhesion Force* (nN)	Adhesion Energy* (fJ)
PMMA	45.77 ± 0.47	1.64 ± 0.01
Silicone	2.10 ± 0.01	0.60 ± 0.01
Hydrophilic acrylic	84.76 ± 0.94	3.49 ± 0.04
Hydrophobic acrylic	283.75 ± 0.14	9.70 ± 0.06

IOL = intraocular lens; PMMA = poly(methyl methacrylate)
*Statistical significance between groups ($P < .001$, ANOVA)

modification in the adhesion was seen with repeated contacts. The AFM imaging confirmed that the IOL surface morphology was not modified or damaged during the force measurements. This test was performed to further verify that adhesion determination was not altered by irreversible changes in the sample.

DISCUSSION

There has been a long debate on theories and techniques to prevent PCO in clinical ophthalmology research. In general, the literature agrees that new surgical techniques and IOL optic designs have contributed to a decrease in the PCO rate in recent years.[2,8] At present, a sharp posterior optic edge is considered to be the major factor in preventing PCO, regardless of the IOL material, because the edge provides a barrier to LECs.[2,14–16,32] This has been verified with different IOL materials, including PMMA, acrylate, and silicone.[21,33,34] On the other hand, the exact influence of the IOL material on PCO prevention is not entirely understood, mainly due to the complexity of managing long-term prospective clinical studies directly comparing the PCO rate after implantation of IOLs of various materials and optic designs.[1–6,17,18,20,35–37]

The adhesiveness of the IOL optic material to the lens capsule has been theorized to be one of the most desirable IOL properties for minimizing PCO. Because the capsular bend requires weeks to form completely,[22,23,38] quick and firm contact between the IOL material and the capsule likely represents the first factor that inhibits the migration of LECs into the space between the IOL and capsule, hastening the capsular bend formation and thus enhancing PCO prevention.

In the past few years, researchers have highlighted the role of the IOL surface adhesion characteristics in influencing the incidence and severity of PCO formation, regardless of the IOL design. Several clinical and experimental studies[37–39] determined qualitatively the adhesion of various IOL materials to the lens capsule, showing stronger adhesion for acrylic IOLs than for PMMA or silicone IOLs. A varying degree of adhesion and migration of LECs onto the IOL surface that was dependent on the IOL material was also found.[20,40–42] To our knowledge, this present study is the first to provide quantitative information on the submicrometer adhesive properties of IOL optics.

As cells move toward a solid surface, the initial interaction between the cell and the biomaterial is governed by long- and medium-range forces, primarily van der Waals and electrostatic, that are strongly dependent on the chemicophysical properties of the respective surfaces. Atomic force microscopy can reliably analyze these surface interactions nondestructively in liquids (ie, in conditions similar to those of the ocular environment) and provide quantitative information on the surface properties of biomaterials with a nanometer-resolved spatial resolution relevant to the size of the interactions between the cells and surface material. Roughness and irregularity are properties that increase the contact surface, making it easier for LECs to migrate on the material. In an earlier AFM study,[24] we found that PMMA IOLs had a higher surface roughness than acrylic or second-generation silicone IOLs. We also found that the optics of the different IOLs had different surface features based on the biomaterial, which is probably dependent on the IOL fabrication processes, and that these features may influence PCO formation.

After determining the surface topography and roughness of IOLs, we focused our research on the adhesive properties of the IOL materials. Atomic force microscopy can further provide valuable information on the nanomechanical properties of solid interfaces such as stiffness and adhesion. The growth of direct force measurements via *f-d* curves obtained by AFM offers new ways to evaluate the biomaterial–aqueous interface.[26–28]

The study of *f-d* curves provided a deeper knowledge of the bioadhesive properties of IOL materials. The measured adhesiveness of the surface optic of acrylic IOLs was stronger than that of the PMMA IOL and silicone IOL, as previously qualitatively argued.[39] In theory, the tacky nature of the acrylic IOL can lead to increased adhesion to the capsule. By binding quickly and tightly to the capsular bag, a more adhesive disk optic may limit LEC migration onto the posterior capsule in the days after surgery, playing a key role in decreasing the rate of PCO.[22,23] In this context, several clinical studies have found a lower incidence of PCO after implantation of acrylic IOLs than of other materials[1,17–19,37] regardless of IOL optic design.

We also found statistically significant differences between hydrophobic and hydrophilic acrylic materials. This could be explained in terms of the hydrophobic effect. In an aqueous environment, hydrophobic interactions usually give the highest adhesion force.[43] The measured difference in surface disk optic adhesiveness between acrylic materials may also play a role in preventing PCO, as clinically reported.[44]

In addition to the type of IOL biomaterial or optic edge design, other factors may influence the cellular behavior at the capsule–lens interface. These include haptic angulation and stiffness, which can actively press the IOL against the capsule; the elasticity and deformation of the capsule itself[45,46]; and the adsorption of extracellular molecules secreted by inflammatory

cells or LECs onto the IOL optic. Indeed, protein molecules have not been shown to play a secondary role in the adhesion mechanism. Linnola et al.[47] hypothesize that if an IOL has more fibronectin bound to it, the IOL can attach to the capsule better because it consists mainly of collagen. Fibronectin was also found to adhere more to hydrophobic acrylic IOLs than to PMMA, silicone, or hydrophilic acrylic IOLs.[48,49]

Another consideration is that IOLs of the same material from different manufacturers can have different surface properties. Using 3 hydrophobic acrylic IOLs, Katayama et al.[49] showed how the adhesiveness of disk optics of the same material and design from a single manufacturer can change significantly because of differences in the surface energy caused by modification of the constituents of the copolymer. It is well known that modifying the surface energy of the IOL optic can influence the adhesiveness of the material.[49,50,51] Further AFM studies that directly compare hydrophobic acrylic IOLs from different manufacturers are needed to confirm this.

In conclusion, the results in this study show the efficacy and accuracy of AFM as a research tool for the analysis of biomaterials that are used in ophthalmology surgical practice. These types of measurements of IOLs can be useful for improving the manufacturing processes and testing experimental approaches to improve biocompatibility and minimize the risk for PCO.[52] Further studies are necessary to elucidate the mechanism of PCO development and the interface interactions between the IOL and capsule.

REFERENCES

1. Findl O, Menapace R, Sacu S, Buehl W, Rainer G. Effect of optic material on posterior capsule opacification in intraocular lenses with sharp-edge optics; randomized clinical trial. Ophthalmology 2005; 112:67–72
2. Kohnen T, Fabian E, Gerl R, Hunold W, Hütz W, Strobel J, Hoyer H, Mester U. Optic edge design as long-term factor for posterior capsular opacification rates. Ophthalmology 2008; 115:1308–1314
3. Mester U, Fabian E, Gerl R, Hunold W, Hütz W, Strobel J, Hoyer H, Kohnen T. Posterior capsule opacification after implantation of CeeOn Edge 911A, PhacoFlex SI-40NB, and AcrySof MA60BM lenses; one-year results of an intraindividual comparison multicenter study. J Cataract Refract Surg 2004; 30:978–985
4. Apple DJ, Peng Q, Visessook N, Werner L, Pandey SK, Escobar-Gomez M, Ram J, Auffarth GU. Eradication of posterior capsule opacification; documentation of a marked decrease in Nd:YAG laser posterior capsulotomy rates noted in an analysis of 5416 pseudophakic human eyes obtained postmortem. Ophthalmology 2001; 108:505–518
5. Hollick EJ, Spalton DJ, Meacock WR. The effect of capsulorhexis size on posterior capsular opacification: one-year results of a randomized prospective trial. Am J Ophthalmol 1999; 128:271–279
6. Sacu S, Menapace R, Wirtitsch M, Buehl W, Rainer G, Findl O. Effect of anterior polishing on fibrotic capsule opacification: three-year results. J Cataract Refract Surg 2004; 30:2322–2327
7. Menapace R, Sacu S, Georgopoulos M, Findl O, Rainer G, Nishi O. Efficacy and safety of capsular bending ring implantation to prevent posterior capsule opacification; three-year results of a randomized clinical trial. J Cataract Refract Surg 2008; 34:1318–1328
8. Findl O, Buehl W, Bauer P, Sycha T. Interventions for preventing posterior capsule opacification. Cochrane Database Syst Rev 2007;(3):CD003738. Available at: http://mrw.interscience.wiley.com/cochrane/clsysrev/articles/CD003738/pdf_fs.html. Accessed February 24, 2009
9. Lois N, Dawson R, McKinnon AD, Forrester JV. A new model of posterior capsule opacification in rodents. Invest Ophthalmol Vis Sci 2003; 44:3450–3457. Available at http://www.iovs.org/cgi/reprint/44/8/3450. Accessed February 23, 2009
10. Majima K, Majima Y. Shape of lens epithelial cells after intraocular lens implantation. J Cataract Refract Surg 2001; 27:745–752
11. Ohnishi Y, Yoshitomi T, Sakamoto T, Fujisawa K, Ishibashi T. Evaluation of cellular adhesions on silicone and poly(methyl methacrylate) intraocular lenses in monkey eyes; an electron microscopic study. J Cataract Refract Surg 2001; 27:2036–2040
12. Müllner-Eidenböck A, Amon M, Schauersberger J, Kruger A, Abela C, Petternel V, Zidek T. Cellular reaction on the anterior surface of 4 types of intraocular lenses. J Cataract Refract Surg 2001; 27:734–740
13. Abela-Formanek C, Amon M, Schild G, Schauersberger J, Heinze G, Kruger A. Uveal and capsular biocompatibility of hydrophilic acrylic, hydrophobic acrylic, and silicone intraocular lenses. J Cataract Refract Surg 2002; 28:50–61
14. Buehl W, Findl O, Menapace R, Rainer G, Sacu S, Kiss B, Petternel V, Georgopoulos M. Effect of an acrylic intraocular lens with a sharp posterior optic edge on posterior capsule opacification. J Cataract Refract Surg 2002; 28:1105–1111
15. Nagamoto T, Fujiwara T. Inhibition of lens epithelial cell migration at the intraocular lens optic edge; role of capsule bending and contact pressure. J Cataract Refract Surg 2003; 29:1605–1612
16. Nishi O, Nishi K, Wickström K. Preventing lens epithelial cell migration using intraocular lenses with sharp rectangular edges. J Cataract Refract Surg 2000; 26:1543–1549
17. Li N, Chen X, Zhang J, Zhou Y, Yao X, Du L, Wei M, Liu Y. Effect of AcrySof versus silicone or polymethyl methacrylate intraocular lens on posterior capsule opacification. Ophthalmology 2008; 115:830–838
18. Hollick EJ, Spalton DJ, Ursell PG, Pande MV, Barman SA, Boyce JF, Tilling K. The effect of polymethylmethacrylate, silicone, and polyacrylic intraocular lenses on posterior capsular opacification 3 years after cataract surgery. Ophthalmology 1999; 106:49–54; discussion by RC Drews, 54–55
19. Wejde G, Kugelberg M, Zetterström C. Posterior capsule opacification: comparison of 3 intraocular lenses of different materials and design. J Cataract Refract Surg 2003; 29:1556–1559
20. Schauersberger J, Amon M, Kruger A, Abela C, Schild G, Kolodjaschna J. Lens epithelial cell outgrowth on 3 types of intraocular lenses. J Cataract Refract Surg 2001; 27:850–854
21. Nishi O, Nishi K, Osakabe Y. Effect of intraocular lenses on preventing posterior capsule opacification: design versus material. J Cataract Refract Surg 2004; 30:2170–2176
22. Nishi O, Nishi K. Effect of the optic size of a single-piece acrylic intraocular lens on posterior capsule opacification. J Cataract Refract Surg 2003; 29:348–353
23. Nishi O, Nishi K, Akura J. Speed of capsular bend formation at the optic edge of acrylic, silicone, and poly(methyl methacrylate) lenses. J Cataract Refract Surg 2002; 28:431–437

24. Lombardo M, De Santo MP, Lombardo G, Barberi R, Serrao S. Analysis of intraocular lens surface properties with atomic force microscopy. J Cataract Refract Surg 2006; 32:1378–1384
25. Yamakawa N, Tanaka T, Shigeta M, Hamano M, Usui M. Surface roughness of intraocular lenses and inflammatory cell adhesion to lens surfaces. J Cataract Refract Surg 2003; 29:367–370
26. Cappella B, Baschieri P, Frediani C, Miccoli P, Ascoli C. Force-distance curves by AFM; a powerful technique for studying surface interactions. IEEE Eng Med Biol 1997; 16(2):58–65
27. Butt H-J, Cappella B, Kappl M. Force measurements with the atomic force microscope: technique, interpretation and applications. Surf Sci Rep 2005; 59:1–152
28. Hodges CS. Measuring forces with the AFM: polymeric surfaces in liquids. Adv Colloid Interface Sci 2002; 99:13–75
29. Vinogradova OI, Butt H-J, Yakubov GE, Feuillebois F. Dynamic effects on force measurements. I. Viscous drag on the atomic force microscopy cantilever. Rev Sci Instrum 2001; 72:2330–2339
30. Hues SM, Draper CF, Lee KP, Colton RJ. Effect of PZT and PMN actuator hysteresis and creep on nanoindentation measurements using force microscopy. Rev Sci Instrum 1994; 65:1561–1565
31. Cappella B, Stark W. Adhesion of amorphous polymers as a function of temperature probed with AFM force-distance curves. J Colloid Interface Sci 2006; 296:507–514
32. Nishi O, Yamamoto N, Nishi K, Nishi Y. Contact inhibition of migrating lens epithelial cells at the capsular bend created by a sharp-edged intraocular lens after cataract surgery. J Cataract Refract Surg 2007; 33:1065–1070
33. Buehl W, Findl O. Effect of intraocular lens design on posterior capsule opacification. J Cataract Refract Surg 2008; 34:1976–1985
34. Kruger AJ, Schauersberger J, Abela C, Schild G, Amon M. Two year results: sharp versus rounded optic edges on silicone lenses. J Cataract Refract Surg 2000; 26:566–570
35. Findl O, Menapace R, Sacu S, Buehl W, Rainer G. Effect of optic material on posterior capsule opacification in intraocular lenses with sharp-edge optics; randomized clinical trial. Ophthalmology 2005; 112:67–72
36. Hayashi K, Hayashi H. Influence on posterior capsule opacification and visual function of intraocular lens optic material. Am J Ophthalmol 2007; 144:195–202
37. Hollick EJ, Spalton DJ, Ursell PG, Pande MV. Lens epithelial cell regression on the posterior capsule with different intraocular lens materials. Br J Ophthalmol 1998; 82:1182–1188
38. Sacu S, Findl O, Linnola RJ. Optical coherence tomography assessment of capsule closure after cataract surgery. J Cataract Refract Surg 2005; 31:330–336
39. Oshika T, Nagata T, Ishii Y. Adhesion of lens capsule to intraocular lenses of polymethylmethacrylate, silicone, and acrylic foldable materials: an experimental study. Br J Ophthalmol 1998; 82:549–553
40. Hesse Y, Kampmeier J, Lang GK, Baldysiak-Figiel A, Lang GE. Adherence and viability of porcine lens epithelial cells on three different IOL materials in vitro. Graefes Arch Clin Exp Ophthalmol 2003; 241:823–826
41. Kurosaka D, Obasawa M, Kurosaka H, Nakamura K. Inhibition of lens epithelial cell migration by an acrylic intraocular lens in vitro. Ophthalmic Res 2002; 34:29–37
42. Versura P, Torreggiani A, Cellini M, Caramazza R. Adhesion mechanisms of human lens epithelial cells on 4 intraocular lens materials. J Cataract Refract Surg 1999; 25:527–533
43. Israelachvili JN. Intermolecular and Surface Forces, with Applications to Colloidal and Biological Systems 2nd ed. San Diego, CA, Academic Press, 1992; 128–131
44. Scaramuzza A, Fernando GT, Crayford BB. Posterior capsular opacification and lens epithelial cell layer formation: Hydroview hydrogel versus AcrySof acrylic intraocular lenses. J Cataract Refract Surg 2001; 27:1047–1054
45. Boyce JF, Bhermi GS, Spalton DJ, El-Ostra AR. Mathematical modeling of the forces between an intraocular lens and the capsule. J Cataract Refract Surg 2002; 28:1853–1859
46. Pedrigi RM, David G, Dziezyc J, Humphrey JD. Regional mechanical properties and stress analysis of the human anterior lens capsule. Vision Res 2007; 47:1781–1789
47. Linnola RJ, Sund M, Ylönen R, Pihlajaniemi T. Adhesion of soluble fibronectin, laminin, and collagen type IV to intraocular lens materials. J Cataract Refract Surg 1999; 25:1486–1491
48. Linnola RJ, Werner L, Pandey SK, Escobar-Gomez M, Znoiko SL, Apple DJ. Adhesion of fibronectin, vitronectin, laminin, and collagen type IV to intraocular lens materials in pseudophakic human autopsy eyes. Part 1: histological sections. J Cataract Refract Surg 2000; 26:1792–1806
49. Katayama Y, Kobayakawa S, Yanagawa H, Tochikubo T. The relationship between the adhesion characteristics of acrylic intraocular lens materials and posterior capsule opacification. Ophthalmic Res 2007; 39:276–281
50. Burnham NA, Dominguez DD, Mowery RL, Colton RJ. Probing the surface forces of monolayer films with atomic-force microscopy. Phys Rev Lett 1990; 64:1931–1934
51. Yuen C, Williams R, Batterbury M, Grierson I. Modification of the surface properties of a lens material to influence posterior capsular opacification. Clin Exp Ophthalmol 2006; 34:568–574
52. Saika S. Relationship between posterior capsule opacification and intraocular lens biocompatibility. Prog Retin Eye Res 2004; 23:283–305

First author:
Marco Lombardo, MD, PhD

Vision Engineering, Rome, and Reggio Calabria, CEMIF. CAL, CNR-INFM LiCryL Laboratory, Physics Department, University of Calabria, Rende, Italy